Science of the Total Environment 496 (2014) 668–677

Contents lists available at ScienceDirect

Science of the Total Environment

journal homepage: www.elsevier.com/locate/scitotenv

Spatial distribution and accumulation of Hg in soil surrounding a Zn/Pb smelter

Qingru Wu [a,b], Shuxiao Wang [a,b,*], Long Wang [a,b], Fang Liu [a,b], Che-Jen Lin [c], Lei Zhang [a,b], Fengyang Wang [a,b]

[a] State Key Joint Laboratory of Environmental Simulation and Pollution Control, School of Environment, Tsinghua University, Beijing 100084, China
[b] State Environmental Protection Key Laboratory of Sources and Control of Air Pollution Complex, Beijing 100084, China
[c] Department of Civil Engineering, Lamar University, Beaumont, TX 77710, USA

HIGHLIGHTS

- Impact of Hg emission from a Zn/Pb smelter was quantified using an integrated model.
- The smelter emission caused 6450 μg m^{-2} yr^{-1} of Hg deposition during 1960–1990.
- Only 14% of Hg emission deposited locally and most emission went into the global pool.
- Hg emission from the smelter increased Hg content in soil from 0.12 to 1.77 mg kg^{-1}.
- The integrated model can be used to assess the impacts of other heavy metals.

GRAPHICAL ABSTRACT

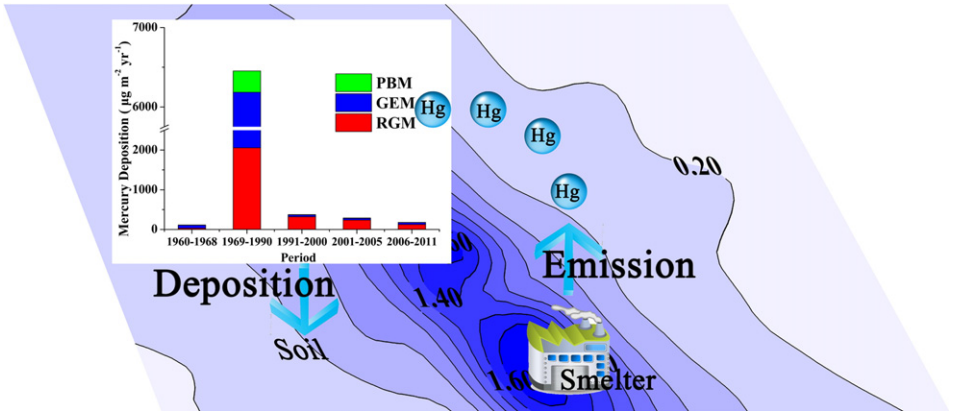

ARTICLE INFO

Article history:
Received 3 October 2013
Received in revised form 8 February 2014
Accepted 9 February 2014
Available online 4 March 2014

Keywords:
Hg emission
Nonferrous metal smelters
Soil contamination
Integrated modeling

ABSTRACT

Nonferrous metal smelting is an important atmospheric mercury (Hg) emission source that has significant local and global impacts. To quantify the impact of Hg emission from non-ferrous metal smelter on the surrounding soil, an integrated model parameterizing the processes of smelter emission, air dispersion, atmospheric deposition and Hg accumulation in soil was developed. The concentrations of gaseous elemental Hg (GEM) around the smelter and the spatial distribution of Hg in the surrounding soil were measured and compared with the model results. Atmospheric deposition of Hg emitted from the smelter was identified as the main source of Hg accumulation in the surrounding soil. From 1960 to 2011, the smelter emitted approximately 105 t of Hg into the atmosphere, of which 15 t deposited locally and resulted in an increase of Hg concentration in soil from 0.12 to 1.77 mg kg^{-1}. A detailed examination of wind rose and model data suggested that the area within 1.0–1.5 km northwest and southeast of the smelter was most severely impacted. It was estimated that the smelter operation from 1969 to 1990, when large scale emission controls were not implemented, resulted in 6450 μg m^{-2} yr^{-1} of Hg net deposition and a model simulated increase of 0.40 mg kg^{-1} of Hg accumulation in the soil. During the period from 1991 to 2011, atmospheric Hg emission from the smelter alone increased the average concentration

* Corresponding author at: State Key Joint Laboratory of Environmental Simulation and Pollution Control, School of Environment, Tsinghua University, Beijing 100084, China. Tel.: +86 1062771466; fax: +86 1062773597.
E-mail address: shxwang@tsinghua.edu.cn (S. Wang).

http://dx.doi.org/10.1016/j.scitotenv.2014.02.067

in soil from 0.41 mg kg^{-1} to 0.45 mg kg^{-1}. In the past 50 years, over 86% of Hg emitted from this smelter went into the global pool, indicating the importance of controlling Hg emissions from non-ferrous metal smelters.

1. Introduction

Mercury (Hg) emissions are a global problem that has no national or continental boundaries. Hg emitted to the atmosphere can travel thousands of miles before it is eventually deposited back to the earth in rainfall or in dry gaseous form. Non-ferrous metal production contributed 15.5% of the Hg emission into the atmosphere globally (UNEP, 2013). In China, non-ferrous metal smelting contributed about 40–45% of national atmospheric Hg emission from 1996 to 2003 (Wu et al., 2006). Recent study indicates that atmospheric Hg emissions from Chinese zinc (Zn), lead (Pb) and copper (Cu) smelters were 73 t in 2010 (Wu et al., 2012). Atmospheric Hg emissions from nonferrous metal smelters cause not only atmospheric pollution but also severe soil pollution (Ettler et al., 2007; Feng et al., 2006; Kalac et al., 1991; Kalac et al., 1996; Li et al., 2011; Lin et al., 2012; Rieuwerts and Farago, 1996; Svoboda et al., 2000; Yin et al., 2009). Mercury concentration in soil up to 2.32 mg kg^{-1} has been observed in a historic Pb mining and smelting town in the Czech Republic (Rieuwerts and Farago, 1996). In China, the soil Hg content was found to be as high as 0.86 mg kg^{-1} in artisanal Zn smelting areas of Guizhou Province (Feng et al., 2006). The Hg concentrations in soil near large-scale industrial smelters were at the range of 0.05–14.60 mg kg^{-1} for Huludao (Zheng et al., 2011), and 0.15–2.89 mg kg^{-1} for Zhuzhou (Li et al., 2011). In the vicinity of secondary Cu smelters in Zhejiang Province, the highest Hg concentration in soil reached 15.01 mg kg^{-1} (Yin et al., 2009). However, the mean Hg concentration was 0.04 mg kg^{-1} in Chinese background soils (Wei et al., 1991). Total Hg concentrations in the soil of Chinese remote sites were generally less than 0.20 mg kg^{-1} (Zhang et al., 2002; Liu et al., 2003, 2006; Wang et al., 2009).

On-site measurements are usually conducted to assess the Hg contamination near large point sources including non-ferrous metal smelters. However, this method requires a large number of samples to account for the large variation of Hg concentrations in the soil near smelters. Additionally, smelters are often located in industrial complexes in China, which means that other potential industrial sources may also influence soil Hg concentrations. Because of this, on-site measurements are not capable of quantifying the contribution of the target sources to the Hg contamination of surrounding soil. Moreover, the observed concentrations in the soil could reflect the pollution levels when the on-site measurements were conducted, but they are not an adequate record of historical concentration change. Integrated methods which combined the plume/puff model and the watershed/lake model were used to quantify the Hg input to a lake caused by emissions of power plant (US EPA, 1997). This approach was applied to assess the impact of waste gasification on surrounding human health (Lonati and Zanoni, 2013). However, the models used in these studies were not effectively evaluated in terms of input parameters and model outputs before they were applied to assess the impact of Hg on local environment as well as on human health risk. Such method integrating emission and pollution is rarely used for smelters because of the lack of important input parameters such as emission rate. We hypothesize that use of data from recent field experiments on atmospheric Hg emissions from nonferrous metal smelters (Li et al., 2010; Wang et al., 2010; Zhang et al., 2012b), and observations of concentrations in air and soil will provide a foundation for an integrated model that will allow for estimation of emissions from large point sources to Hg soil pollution.

In this study, an integrated approach assessing the input of Hg emissions from large point sources to the Hg soil pollution and the subsequent accumulation in the soil was developed. The model components include emission module, Gaussian plume dispersion module, dry and wet deposition module, and module for Hg accumulation in the soil. The developed model was adopted to assess the impact of Hg emissions from a Zn/Pb smelter to Hg contamination of the soil in surrounding areas. Concentrations of gaseous elemental Hg (GEM) around the smelter and the Hg distribution in the surrounding soil were measured to evaluate model results. The accumulation and spatial distribution of Hg in the soil were further quantified based on model simulations. The integrated model developed in this study can be used to assess the impact of Hg as well as other metals from large point sources to their surrounding environment.

2. Methodology

2.1. Site description and study domain

The Zn/Pb smelter is located in the northwest quadrant of Zhuzhou City, Hunan Province, China (Fig. 1). The smelter underwent 5 major operational changes in terms of production capacity and the implementation of air pollution control devices (APCDs) (Table 1). Currently, the smelter operates 1 Pb production line (Pb1) and 2 Zn production lines (Zn1 and Zn2). The Pb production line is operated with a sinter machine process. During this process, Pb concentrates are firstly dried in the dehydration kiln before being roasted in a sinter machine to produce Pb calcine. The Pb calcine is further converted in the blast furnace to produce crude Pb, which is 95–99% pure. The crude Pb is then refined to remove impurities in the refining process. Since the crude Pb contains little Hg, atmospheric Hg emission from refining process can be ignored. The exhausted gas is emitted from 1 stack for dehydration kiln flue gas (Pb1P1), 1 stack for sinter flue gas (Pb1P2), and 1 stack for blast furnace flue gas (Pb1P3). The 2 Zn production lines are electrolytic processes. During this process, the Zn concentrates are firstly dried in the dehydration kilns, and then roasted. The Zn calcine produced by the roasters is then leached in the leaching process. The leachate is purified and electrolyzed to produce refined Zn while the leaching sludge is sent to volatilizing kilns to reclaim refined Zn. In the Zn producing process, atmospheric Hg is emitted from the stacks for the dehydration kiln flue gas (Zn1P1 or Zn2P1), roaster flue gas (Zn1P2 or Zn2P2) and volatilizing kiln flue gas (Zn1P3 or Zn2P3). The characteristics of the 9 stacks are shown in Table 2.

The simulation domain (10 km by 10 km, Fig. 1) was divided into 400 cells (500 m spatial resolution). The site is located at a flat terrain with 70% of the area used as cropland. There are industrial areas in the east and southeast quadrants of the domain. The study area has a northerly subtropical monsoon climate with the perennial dominant wind from north–northwest (NNW) except in summer when the wind is primarily from the southeast (SE). The average annual temperature and precipitation is 17.5 °C and 1400 mm, respectively, according to the data from the CMDSSS (China Meteorological Data Sharing Service System, available at http://cdc.cma.gov.cn/home.do, last accessed on January 14, 2014). The weather conditions with unstable atmospheric stability occur less than 5% of the time.

2.2. Model development

An integrated model assessing the emission transport from large point source deposition and the subsequent accumulation in the soil was developed. The model components include emission estimation, Gaussian plume dispersion, dry and wet deposition, and Hg accumulation in the soil.

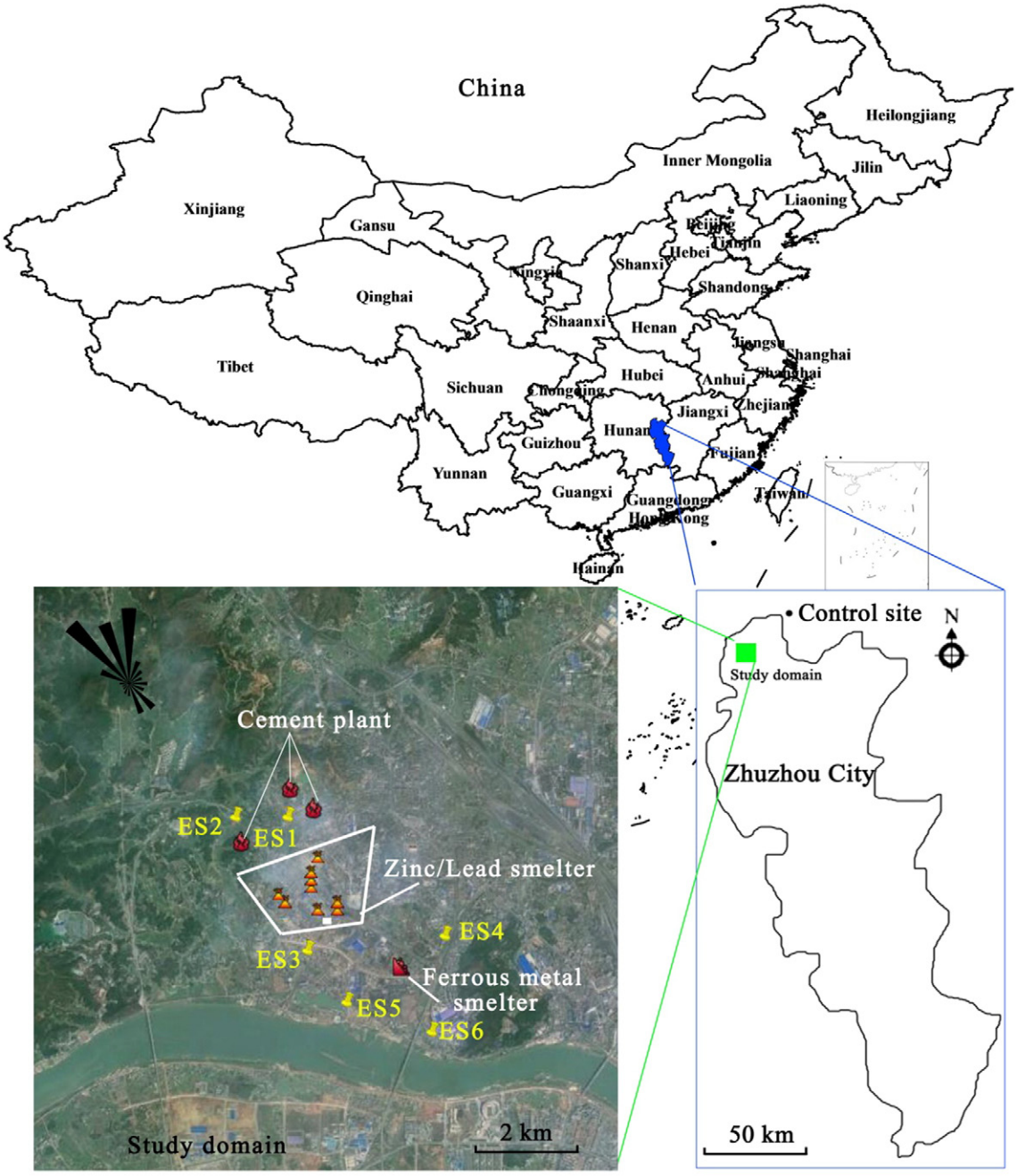

Fig. 1. Study domain and location of industrial facilities located in the northwest quadrant of Zhuzhou City, Hunan Province, China. (The wind rose shows the annual average frequency with which the wind blows from a given direction.)

2.2.1. Emission estimation

The emission estimation included the non-ferrous metal smelter metal purification process from ore through dehydration, roasting, extraction, and the reclaiming processes. During these processes, Hg in ore concentrates is released as gaseous Hg in the flue gas. The released gaseous Hg was directly emitted to the atmosphere during the period from 1960 to 1968 (Table 1). The dust collectors (DC) were installed to remove fly ash in 1969 and acid plants (AP) were installed to recover SO_2 in 1991. In these processes, part of the Hg would be transferred into fly ash, waste water, and sulfuric acid (Table 1). Two Hg reclaim towers were installed to recycle Hg in the 2 Zn smelting lines respectively so as to minimize Hg emission (Table 1). In this study, an emission module similar to the technology-based model by Wu et al. (2012) was developed. The model for national emission estimation provided by Wu et al. (2012) was adjusted according to the technology adopted in the studied smelter. In addition, fugitive Hg emissions were added to the emission module, which was not considered in the research of Wu et al. (2012).

The emission mass flow rate Q (g s^{-1}) from stacks for speciated Hg was calculated as follows:

Emission rate from stacks for the dehydration kiln (d) is

$$Q_{di} = \theta_{di} \frac{CM\gamma_d(1-\eta_d)}{365 \times 24 \times 3600}; \quad \text{(E1)}$$

emission rate from stacks for the sinter/roaster (s) is

$$Q_{si} = \theta_{si} \frac{CM(1-\gamma_d)\gamma_s(1-\eta_s)}{365 \times 24 \times 3600}; \quad \text{(E2)}$$

Table 1
The developing history of the smelter.

Period	Zinc producing lines (Zn1 & Zn2)			Lead producing line (Pb1)			Total Hg emitted from smelter (t)	Total Hg accumulated in soil (t)
	Production (kt yr^{-1})	Ore consumption (kt yr^{-1})	APCDs[a]	Production (kt yr^{-1})	Ore consumption (kt yr^{-1})	APCDs[a]		
1960–1968[c]		–	–	20	34	None	2	0.1
1969–1990	100	208	DC	30	50	DC	95	14.2
1991–2000	170	350	DC + AP_d	70	120	DC + AP_s	3	0.4
2001–2005	450	930	DC + AP_d/DC + AP_d + RT[b]	100	170	DC + AP_s	3	0.1
2006–2011	500	1040	DC + AP_d + RT	100	170	DC + AP_s	2	0.1

[a] Air pollution control devices for smelting flue gas. None — no air pollution control devices; DC — dust collector; AP_d — acid plants with double conversion and double absorption tower; AP_s — acid plants with single conversion and single absorption tower; RT — Hg reclaim tower.
[b] During 2001–2005, about 60% of smelting flue gas from zinc smelter was treated with AP_d + RT.
[c] The lead line was operated in August of 1959. Considering the unstable production in that year, we have not considered its impact in this study.

emission rate from stacks for the blast furnace (e) is

$$Q_{ei} = \theta_{ei}\frac{CM(1-\gamma_d)(1-\gamma_s)\gamma_e(1-\eta_e)}{365\times 24\times 3600}; \quad \text{(E3)}$$

emission rate from stacks for the volatilizing kiln (r) is

$$Q_{ri} = \theta_{ri}\frac{CM(1-\gamma_d)(1-\gamma_s)(1-\gamma_e)\gamma_r(1-\eta_r)}{365\times 24\times 3600} \quad \text{(E4)}$$

where i denotes Hg species. d, s, and e stand for dehydration, roasting and blasting, respectively. M and C are annual ore consumption (t yr^{-1}) (Table 1) and Hg concentration (mg kg^{-1}). The mean concentration in Zn concentrates processed by the smelter was 41.3 mg kg^{-1} (Wang et al., 2010); the mean concentration in Pb concentrates was 10.1 mg kg^{-1} (Wu et al., 2012). The γ is the Hg release ratio (%), which is the percentage of Hg released from the input materials into the flue gas (0.8%–99.4% for the dehydration kilns, roasters and volatilization kilns in the Zn production line and 0.1%–98.7% for the dehydration kiln, sinter, and blast furnace in the Pb production line, Table 3); η is Hg removal efficiency (%, Table 3). Hg removal efficiency depends on the application of APCDs (Wang et al., 2010; Li et al., 2010; Zhang et al., 2012b). The Hg in flue gas includes GEM, reactive gaseous Hg (RGM), and particulate bound Hg (PBM), and θ is the percentage of each Hg species (%) in the emitted flue gas. The Hg speciation percentage in the emitted flue gas after acid plant was measured by Wang et al. (2010). The percentage of Hg species emitted from the dehydration and volatilizing/fuming furnaces was based on Li et al. (2010) and Zhang et al. (2012b). For flue gas from AP, RGM constituted 88%; while it only accounted for 15–21% in the roasting flue gas (Table 3). In the 5 different stages of operation, the percentage of GEM in dehydration, blasting and volatilizing flue gas contributed 50–80% of total emissions (Table 3).

Fugitive Hg emission refers to the Hg emitted from Hg-containing materials into the atmosphere when these were stored in uncovered piles. The emission mass flow rate Q_f (g s^{-1}) for fugitive Hg emission from the sludge of flue gas scrubber, and electrostatic demister waste water was calculated according to the method described in the study of Wang (2010). With this method, fugitive emission rate was calculated as the product of the concentration difference measured upwind and downwind of the sludge pile, wind speed and cross-sectional area of sludge pile against wind direction. The fugitive Hg emission was assumed to be GEM. The difference between the GEM concentrations downwind and upwind was assumed to be caused by the fugitive emission from the sludge. The concentrations of the GEM both downwind and upwind of the sludge pile were measured by Lumex® RA-915M analyzer 3 times a day (at least 1 h each time) and repeated for 3 days. The 30 s average concentration of GEM downwind reached as high as 20 μg m^{-3}, with an hourly average of 1 μg m^{-3} while the hourly average concentration upwind was 15 ng m^{-3}. The quality assessment and quality control of this equipment are discussed in Section 2.3.1.

There are other Hg emission sources in the industrial complex, including 3 cement plants and 1 ferrous metal smelter (Fig. 1). The annual production capacities of the 3 cement plants were 200 kt, 88 kt and 88 kt, respectively. The capacity of the metal smelter was 100 kt yr^{-1}. The emission factors of 0.065 g t^{-1} and 0.04 g t^{-1} were adopted for the cement plants and metal smelter (Wang et al., 2006). The emission speciation of these 2 sources was assumed to be 85% GEM, 15% RGM and 5% PBM (Wang et al., 2006).

2.2.2. Air dispersion

The air dispersion module estimates atmospheric Hg concentration at ground level. The air dispersion was simulated using a Gaussian dispersion model: the industrial source complex (ISC) model. Although there are several updated puff/plume models such as AERMOD (AMS/EPA regulatory model) and CALPUFF (Lagrangian puff dispersion model), we chose the ISC model considering the model applicability in the study domain and the input data availability. The ISC model accepts hourly meteorological data records to define the conditions for plume rise, transport, diffusion, and deposition. The model estimates the concentration or deposition of gases and particles for each hour of input meteorology. The atmospheric concentration of speciated Hg (C_g) was calculated based on the speciated Hg emission rates, stack characteristics (Table 2) and meteorological data. The modeling period was from 1960 to 2011. The hourly wind speed (m s^{-1}), wind direction (°), ambient temperature (K), precipitation amount (mm), radiation levels (W m^{-2}), and dew point temperature (K) for the period from 2001 to 2011 were obtained from the CMDSSS. Due to the lack of observed meteorology, the same meteorological data was used for the years between 1960 and 2001. The joint frequency of wind speed, wind direction, and stability was calculated based on the meteorological data during 2001–2011. Other parameters including temperature, mixing layer heights, and surface roughness applied were the monthly average of the data during 2001–2011. The ISC model uses the mixing height to reflect dispersion characteristics. The mixing height was calculated according to the standard methods of GB/T 13201-91 (MEP, 1991). This method calculated the mixing height according to the different formulas under different atmospheric stability classes. The atmospheric stability class was determined according to solar elevation angle, cloud cover, and wind speed.

2.2.3. Deposition

The total deposition flux F_t, calculated as the sum of dry (F_{dry}) and wet (F_{wet}) deposition, was calculated for each Hg species as:

$$F_{i,t} = F_{i,dry} + F_{i,wet} = A_{dry}\times C_{g,i}\times V_{i,d} + A_{wet}\times C_{l,i}\times P \quad \text{(E5)}$$

where F is the deposition flux (μg m^{-2} yr^{-1}), i is the Hg speciation, and t refers to the total deposition. A_{dry} and A_{wet} are unit conversion factors (315.16 m s μg ng^{-1} cm^{-1} yr^{-1} and 0.001 μg ng^{-1}), C_g is the atmospheric Hg concentration from the dispersion module (ng m^{-3}), and V is the species-specific dry deposition velocity (cm s^{-1}) calculated by

Table 2
Characteristics of the 9 stacks studied including height, exit temperature, velocity, and diameter.

Stack number	Description	Stack height (m)	Exhaust gas temperature (K)	Exit velocity (m s^{-1})	Stack diameter (m)
Pb1P1	Stack for the dehydration kiln of NO.1 lead producing line	30	325	25	1.0
Pb1P2	Stack for the d sinter of NO.1 lead producing line	120	325	15	1.6
Pb1P3	Stack for the blast furnace of NO.1 lead producing line	120	355	25	1.0
Zn1P1	Stack for the dehydration kiln of NO.1 zinc producing line	30	325	25	1.0
Zn1P2	Stack for the roaster of NO.1 zinc producing line	120	330	15	1.6
Zn1P3	Stack for the volatilization kiln of NO.1 zinc producing line	35	316	25	1.0
Zn2P1	Stack for the dehydration kiln of NO.2 zinc producing line	30	325	25	1.0
Zn2P2	Stack for the roaster of NO.2 zinc producing line	120	330	15	1.6
Zn2P3	Stack for the volatilization kiln of NO.2 zinc producing line	40	316	25	1.0

the meteorology chemistry interface processor (MCIP) version 3.6 (Byun and Ching, 1999). In the MCIP, the dry deposition velocities of GEM and RGM are calculated using a resistance deposition scheme (Wesely, 1989). The dry deposition velocity of PBM was calculated explicitly, similar to that of fine aerosols in Aitken and Accumulation models (Binkowski and Roselle, 2003).

The land use data applied for the MCIP were based on those from the United States Geological Survey (USGS). The land use categories in the study domain included dry land and cropland, irrigated cropland, cropland–grassland mosaic, grassland, shrub land, water, and urban land, which accounted for 7.8%, 31.4%, 31.2%, 8.7%, 0.8%, 7.9%, and 12.2% of the total area in our study domain, respectively. The MCIP was driven by meteorological fields generated by the Weather Research and Forecasting Model (WRF version 3.3). The meteorological parameters simulated by the WRF were evaluated by the observed data obtained from the CMDSSS. Wind speed, temperature and humidity of 2006 and 2011 were chosen for comparison. The monthly observed and simulated concentrations were used to calculate the bias and gross errors which were adopted as the statistical indices. The benchmarks for the bias and gross errors were from the suggestion of Emery et al. (2001). The biases of monthly average wind speed were below the benchmarks of ± 0.5 m s^{-1}. The biases of wind speeds for Feb–May 2006 were slightly above the benchmark (0.51–0.57 m s^{-1}). The temperature and humidity were reproduced well, with bias less than ± 0.5 K and ± 1 g kg^{-1}. The gross errors for the three meteorology indices in all months were less than the benchmarks (2 m s^{-1}, 2 K and 2 g kg^{-1}), respectively. Generally speaking, these data indicate a relatively good performance of meteorological prediction. The parameter C_l in the flux equation is aqueous oxidized Hg concentration in the dissolved or sorbed phase (ng m^{-3}). RGM is highly soluble in water and was assumed to be completely scavenged into the aqueous phase during precipitation events. For PBM, C_l was estimated by the fraction of PBM scavenged by washout using the method adopted in GEOS-Chem (Liu et al., 2001). P is precipitation intensity (m yr^{-1}).

2.2.4. Accumulation in soil

The total Hg concentration in the soil was estimated using the simulated atmospheric deposition and the estimated loss of Hg from soil through leaching, runoff and volatilization (US EPA, 2005):

$$C_{so} = \frac{\sum_i F_{i,t}[1-\exp(-k_{so}\cdot T)]}{Z_{so}\cdot k_{so}\cdot BD} \quad \text{(E6)}$$

where i is the Hg speciation, t refers to total deposition, C_{so} is the simulated Hg concentration (mg kg^{-1}) in soil, F is the deposition flux (μg m^{-2} yr^{-1}), Z_{so} is the soil mixing depth (cm), T is the period of smelter operation (yr, Table 1), BD is soil bulk density (g cm^{-3}), and k_{so} is the soil loss constant (yr^{-1}). The US EPA (2005) recommends the value of k_{so} be determined using the characteristics of the soil to estimate the loss resulting from (1) leaching (k_{sg}), (2) erosion (k_{se}), (3) runoff (k_{sr}), (4) biotic and abiotic degradation (k_{sl}), and (5) volatilization (k_{sv}). Here, k_{se} was assumed to be zero because the contaminated soil erodes both onto and off the site according to the US EPA's recommendation. The value for k_{sg} was also set to zero (US EPA, 2005) because of the lack of kinetic data for biotic and abiotic processes in soil. Using these assumptions, the soil loss constant for Hg becomes:

$$kso = ksr + ksl + ksv \quad \text{(E7)}$$

$$k_{sr} = \frac{RO}{\theta_{sw}\cdot Z_{so}}\left(\frac{1}{1+Kd_{so}\cdot BD/\theta_{sw}}\right) \quad \text{(E8)}$$

$$k_{sl} = \frac{P+I-RO-E_v}{\theta_{sw}\cdot Z_{so}\cdot(1+Kd_{so}\cdot BD/\theta_{sw})} \quad \text{(E9)}$$

Table 3
Values applied for specific parameters in the emission model from 1960 to 2011. Processes considered included dehydration, smelting, blasting, and volatilization from ore piles.

Metal type	Parameter	Dehydration		Smelting			Blasting		Volatilizing
		1960–1968	1969–2011	1960–1968	1969–1990	1991–2011	1960–1968	1969–2011	1969–2011
Zinc	Hg release rate, γ (%)[a]	–	0.8	–	99.4	–	–	–	87.2
	Hg removal efficiency, η (%)[a]	–	12.5	–	12.5	99/99.7[c]	–	–	12.5
	Percentage of GEM, θ_{GEM} (%)[b]	–	74	–	74	15	–	–	62
	Percentage of RGM, θ_{RGM} (%)[b]	–	21	–	21	80	–	–	32
	Percentage of PBM, θ_{PBM} (%)[b]	–	5	–	5	5	–	–	6
Lead	Hg release rate, γ (%)[a]	0.1	0.1	98.7	98.7	98.7	58	58	–
	Hg removal efficiency, η (%)[a]	0.0	12.5	0.0	12.5	95.9	0.0	12.5	–
	Percentage of GEM, θ_{GEM} (%)[b]	80	74	80	74	7	50	50	–
	Percentage of RGM, θ_{RGM} (%)[b]	15	21	15	21	88	45	45	–
	Percentage of PBM, θ_{PBM} (%)[b]	5	5	5	5	5	5	5	–

[a] Wu et al. (2012), Zhang et al. (2012b), Wang et al. (2010) and Li et al. (2010).
[b] Wu et al. (2012), Zhang et al. (2012b), Wang et al. (2010), Li et al. (2010) and Streets et al. (2005).
[c] The Hg removal rate reached 99.7 when the reclaim towers were installed.

$$k_{sv} = \frac{A \cdot H}{Z_{so} \cdot Kd_{so} \cdot R \cdot T_a \cdot BD} \cdot \left(\frac{D_a}{Z_{so}}\right) \cdot \left(1 - \frac{BD}{\rho_{soil}} - \theta_{sw}\right). \quad \text{(E10)}$$

The descriptions and values of the variables in E7–E10 are listed in Table 4. Most of the values recommended by the US EPA (2005) were applicable in the domain. The main site-specific parameters were the average annual precipitation (P), average annual surface runoff from pervious areas (RO), average annual irrigation (I), and average annual evaporation (E_v). The average annual precipitation was from the surface observation data at the station for our study sites (CMDSSS). The average annual surface runoff from previous areas and the average annual evaporation for this site were found in the resources of hydrogeology foundation (Wang, 1995). The average annual irrigation was calculated based on the irrigation amount model recommended by Liu et al. (2012).

2.3. Field measurement

2.3.1. Ambient concentration of GEM

The ambient concentrations of GEM were measured from April 22 to May 18, 2012 to examine the performance of the integrated model developed in this study. The observational data were collected at representative locations and time based on the understanding of meteorology. During the sampling period, the dominant wind direction was north–northwest (NNW), and the average wind speed and temperature were 1.63 m s^{-1} and 18.2 °C, respectively. These main meteorology parameters are representative of annual averages with perennial dominant wind of NNW (Fig. 1), annual average wind speed of 1.67 m s^{-1} and annual temperature of 17.5 °C. The sampling sites were also selected at both dominant and non-dominant directions to ensure spatial representativeness. Gaseous elemental Hg concentrations were measured at the six experiment sites (ES1–ES6) where the soil samples were collected and at one control site (Fig. 1). The experiment sampling sites were located within 4 km of the smelter in the dominant wind direction while they were within 1–2 km of the smelter in the non-dominant wind direction (Fig. 1). The control site was located 30 km northeast of the smelter (Fig. 1).

Gaseous elemental Hg was sampled and analyzed using a Lumex® RA-915M analyzer. The analyzer is based on differential Zeeman atomic absorption spectrometry using high frequency modulation of light polarization (ZAAS-HFM). The instrument is calibrated with multiple dilutions of a 1000 μg mL^{-1} certified Hg standard (State Non-ferrous Metals and Electronic Materials Analysis and Testing Center, P/N GSB04-1729-2004) every 12 months and by an internal Hg source every 24 h. The instrument detection limit is 2 ng m^{-3}. Before each measurement, the Lumex RA-915M was operated for 30 min to stabilize (with the drift of blank not more than 2 ng m^{-3} within the last 10 min). During the measurement, all the measurements were conducted at a height of 1.5 m from the ground. The baseline was automatically adjusted every 5 min.

2.3.2. Soil sampling and analysis

Soil samples were collected using a stratified random sampling method (Brus and de Gruijter, 1997; http://www.epa.gov/quality/qksampl.html, last accessed on January 14, 2014). For this method, prior information about the area is used to create groups that are sampled independently using a random process. In this study, the study area was divided into 7 areas based on land usage types. In each area (the land usage type of water was not included), the soil sampling sites were distributed both in dominant wind direction and in non-dominant direction to ensure representativeness (Fig. 1). Soil samples at depths of 0–20 cm and 80–100 cm were collected to represent the polluted soil and the background soil. No less than 5 samples were collected at each site. All samples were air dried to constant weight and then pulverized into a sieve with 80 meshes (200 μm). The soil Hg content was analyzed using the Direct Combustion Method (ASTMD 6722-01) with a Milestone™ DMA-80. The absolute detection limit is 0.02 ng. Multiple dilutions of a 1000 μg ml^{-1} certified Hg standard (State Non-ferrous Metals and Electronic Materials Analysis and Testing Center, P/N GSB04-1729-2004) were used for equipment calibration. Certified reference materials (CRMs, supplied by the National Research Center for CRMs of China, Beijing) were also used as the external standard for every 3 samples. Each sample was analyzed at a minimum of 3 times to obtain parallel results with a relative standard deviation of <5%.

2.3.3. Statistical analysis

Microsoft Excel software (Excel 2010) was applied for statistical analysis and Origin Data analysis and graphing software (OriginPro8.5) was used for figure drawing.

3. Results and discussion

3.1. Mercury emission from the industrial sources

Mercury emissions from the industrial sources in the study domain were estimated to be 0.37 t in 2011. The emissions of GEM, RGM and PBM were estimated to be 0.26 t, 0.09 t and 0.02 t, respectively. The emission of the Zn/Pb smelter, cement plant and primary metal smelter were 0.35 t, 0.02 t and 0.004 t, respectively. The Zn/Pb smelter is the dominant source, contributing 94% of the total emissions.

The uncertainty of the emission of this smelter was estimated by combining the coefficients of variation (CV, or the standard deviation divided by the mean) of the contributing factors according to the

Table 4
Parameters used in equations of E7–E10 to calculate the soil loss constant.

Parameters	Meaning	Value	Unit	Reference
RO	Average annual surface runoff from previous areas	10	cm yr^{-1}	Wang (1995) and Liu et al. (2012)
θ_{sw}	Soil volumetric water content	0.2	ml cm^{-3}	US EPA (2005)
K_{dso}	Soil/water partition coefficient	1000	ml g^{-1}	US EPA (2005)
Z_{so}	Soil mixing zone depth	20/2	cm	US EPA (2005)
BD	Soil bulk density	1.5	g cm^{-3}	US EPA (2005)
P	Average annual precipitation	140	cm yr^{-1}	CMDSSS
I	Average annual irrigation	0	cm yr^{-1}	Wang (1995) and Liu et al. (2012)
E_v	Average annual evaporation	50	cm yr^{-1}	Liu et al. (2012) and CMDSSS
A	Units conversion factor	3.1536×10^7	s yr^{-1}	US EPA (2005)
H	Henry's law constant	0.0071	atm-m^3 mol^{-1}	US EPA (2005)
R	Universal gas constant	8.206×10^{-5}	atm-m^3 mol^{-1} K^{-1}	US EPA (2005)
T_a	Ambient air temperature	291.8	K	US EPA (2005)
D_a	Diffusivity of Hg in air	0.0109	cm^2 s^{-1}	US EPA (2005)

methodology for uncertainty analysis described in Streets et al. (2003). The relative 95% confidence intervals for emissions are calculated as 1.96 times CV. The uncertainty in the emission estimate could result from ore consumption, Hg removal efficiency of APCDs, and Hg concentration in ore. Ore consumption was recorded from the operational data, and the Hg removal efficiency was based on field measurements in the smelter (Wang et al., 2010), which were relatively accurate to a certain extent. Hg concentrations in Zn (41.3 mg kg^{-1}) and Pb (10.1 mg kg^{-1}) concentrates applied were the annual average value. Considering that Hg concentration in the ore consumed by this smelter varied by batches (Fig. 2), this is likely the most important factor causing the uncertainty in Hg emissions. The calculated uncertainty of the emissions of the smelter caused by the uncertainty of Hg concentration in the consumed concentrates was ~30%. The uncertainties for the past years were also assumed to be 30% since there were no historical data available.

3.2. Comparison of simulated and observed concentrations of GEM

The observed mean concentration of GEM at ES1–ES6 ranged from 6.4 to 40.3 ng m^{-3}, with a grand mean of 19.5 ng m^{-3}. The average observation time for ES1–ES3 was 4 days at each site while that for ES4–ES6 and CS was 3 days per site. The concentration of GEM was strongly influenced by anthropogenic emission sources, as evidenced by the dependence of GEM on wind direction at the 6 sites. For example, ES1 is northwest of the smelter. The wind rose (Fig. 3a) combined with the GEM concentration at ES1 (Fig. 3b) showed that the concentration of GEM on Apr 22, Apr 23 and Apr 26 was 4–6 times elevated when ES1 was downwind of the smelter compared to the GEM concentration on Apr 25. The observed regional background concentration at CS site was 5.3 ng m^{-3}, with a range in concentrations from 1.9 to 5.7 ng m^{-3}, similar to that observed in remote areas (Fu et al., 2008, 2010; Wan et al., 2009). Thus, the observed mean concentration at the CS site was used for screening out the background signal.

Both observed and simulated GEM concentrations exhibited large temporal variability (Fig. 4). The large deviation was caused by the combined effect of smelter emission and associated atmospheric processes. The observed mean daily concentration was generally greater than the simulated concentration. About 70% of the simulated GEM concentration is located in 85% of the observed concentration. The underestimation of the simulated GEM concentration could be attributed to

Hypothesis (1). the uncertainties in estimating emission quantity and speciation,

Hypothesis (2). the overestimation of mixing height,

Hypothesis (3). the omission of Hg natural emission,

Hypothesis (4). the uncertainty of Hg chemistry

Hypothesis (5). the overestimation of dry deposition velocity.

The uncertainty in estimating emission quantity is most likely due to Hypothesis (1) the uncertainty in Hg content in ore concentrates. During the simulation, the annual mean Hg concentration was used in the simulation. In practice, the Hg content in ore varies with respect to the batches of ores (Fig. 2). To address such variability, a sensitivity analysis of the emission uncertainty of 30% was assumed. The increased smelter emission had reduced the difference between the observed and simulated GEM concentrations. All the simulated data were within 85% of the observed concentrations and the underestimation of smelter emission quantity can explain this. To evaluate the impact of speciation, the influence of emission speciation was assessed through varying GEM speciation fractions from 74% to 80% (the highest percentage of GEM in total Hg in dehydration flue gas during onsite measurements) in dehydration flue gas, from 7% to 15% in roasting flue gas, and from 50% to 54% in volatilizing flue gas, respectively. Tested results indicated that the increase in GEM percentage had slight improvement on the comparison between simulated and observed concentrations of GEM. The sensitivity of GEM concentrations to mixing height was tested and the results indicated that when decreasing the mixing height by 10%, simulated GEM concentration increased by 1%, 2%, 2%, 6%, 5%, and 5% at ES1–ES6, respectively. Therefore, the mixing height was not the dominant factor resulting to the underestimation of GEM concentration.

Hypotheses (3)–(5) were assessed based on previous studies. Since natural emission is a diffuse source and does not significantly modify the ambient concentration as what was observed (Gbor et al., 2006; Lin et al., 2005), it is unlikely that Hypothesis (3) was the dominant cause for the underestimation of simulated GEM concentration. Hypothesis (4) was not important because of the slow gaseous oxidation kinetics of GEM and the short residence time of Hg in the model domain (<1 h under typical wind condition). Hypothesis (5) is

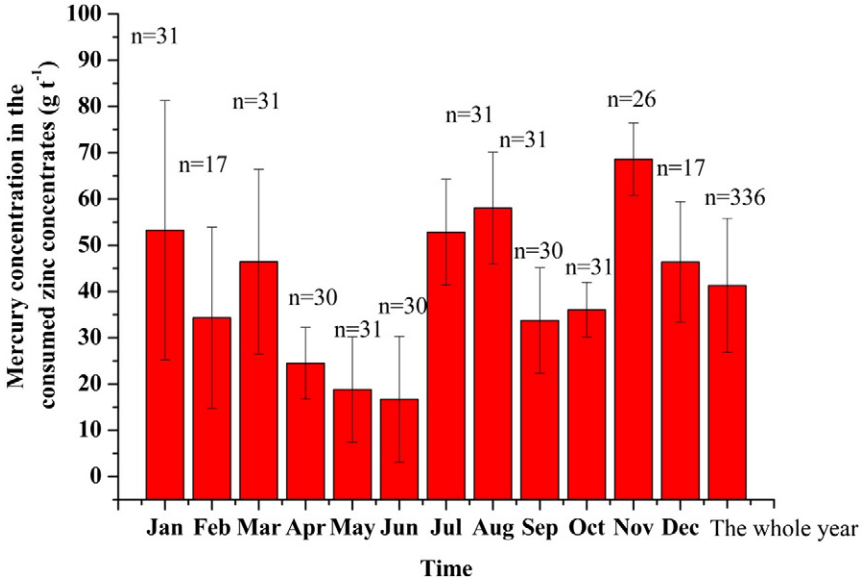

Fig. 2. Mercury concentration in the monthly consumed concentrates during one year sampling period. (The red columns refer to the geometric mean of mercury concentration in the monthly consumed zinc concentrates. The error bar is the standard deviation of mercury concentration. n is the number of batches sampled every month.)

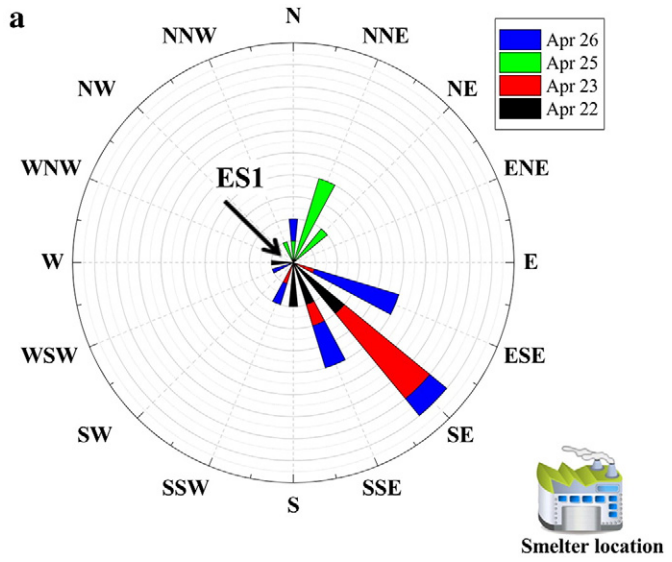

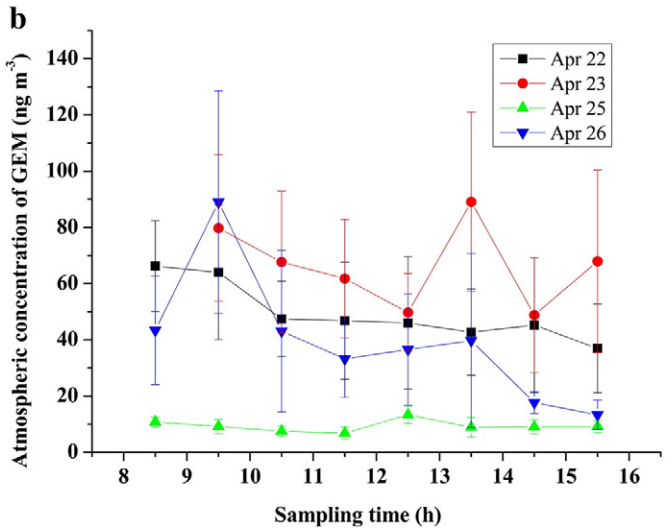

Fig. 3. Wind rose (wind direction distribution on Apr 22, 23, 25, and 26) and concentration of GEM at ES1. The location was chosen based on forecasting. (a) Wind rose (wind direction distribution on Apr 22, 23, 25, and 26). (b) GEM concentration at ES1 during monitoring period. (The error bar at each point represents the standard deviation of observed mercury concentrations.)

regarding overestimation of dry deposition. The dry deposition velocity was the output from the MCIP using a resistance deposition scheme. This method has been evaluated by previous study (Zhang et al., 2012a) and it is believed that the GEM dry deposition velocity is relatively realistic considering that the simulated GEM concentration agreed within as less as 5% of measured concentration at 5 non-urban areas.

Therefore, the most likely cause for the underestimation in GEM concentration was the underestimated Hg concentration in ore concentrates used for the simulation. However, for the long term annual simulation, the model estimated concentration should be representative of GEM concentration.

3.3. Spatial distribution of Hg in soil

Mean Hg concentrations at the 6 sites (0–20 cm depth) ranged from 0.62 to 2.61 mg kg^{-1}, with a mean of 1.54 mg kg^{-1}. Compared to the Hg content (0.11–0.45 mg kg^{-1}) of background soil (80–100 cm depth), the top soil appeared to be contaminated from the atmospheric deposition of Hg caused by the nearby point sources. The simulated concentration agreed with measured concentration (Hg simulation = 0.7

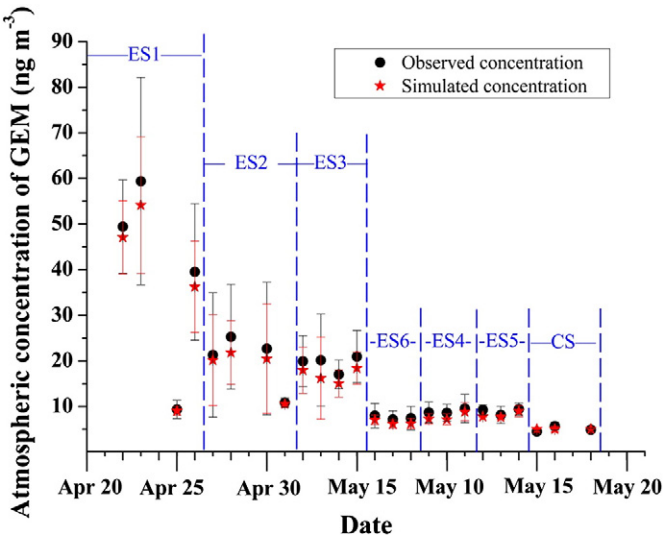

Fig. 4. Comparison of observed and simulated concentrations of GEM. (The error bar at each point represents the standard deviation of observed mercury concentration.)

observation, with $r = 0.95$ and $p < 0.05$). The degree of agreement between the simulated and observed soil Hg concentrations suggested that the model estimates for long-term accumulation from atmospheric deposition were conceivable. The constraint of model results by measurements in both air and soil is robust compared to the approach in typical air dispersion studies where only air concentration is applied to constrain the model results. The model results in this study effectively bridge the gaps of the observational data in this study and demonstrate the benefits of the integrated model.

Despite potential contribution from other sources, we estimated that 73–92% of Hg in the soil at the experiment sites was from the non-ferrous metal smelter. Simulation results indicated that Hg concentration in soil increased from 0.12 mg kg^{-1} to 1.77 mg kg^{-1} in the study domain (Fig. 5). The most severely impacted area was 1.0 km to 1.5 km northwest and southeast of the smelter. Forty percent of the collected top soil samples at those sites have a Hg content classified as highly contaminated (>1.50 mg kg^{-1}) according to China's soil pollution standard (soil environmental quality standards, GB15618-1995). Soil in the northeast and southwest of the domain was less impacted by the smelter, based on the soil Hg data (as low as 0.20 mg kg^{-1}).

3.4. Hg accumulation in soil

The contribution of smelter emissions to the surrounding soil can be correlated with the year when the Pb production line started operating. From 1960 to 2011, the Zn/Pb smelter emitted approximately 105 t of Hg into the atmosphere. Considering both the deposition and re-emission of Hg, we estimated that the emissions led to 15 t of net Hg accumulation in the soil of study domain. Dry deposition contributed 62% of the Hg accumulation in soil, and GEM was the dominant deposition species. Since the concentrate consumption and the APCDs drastically changed from 1960 to 2011, the changed Hg emission rate of this smelter has had a significant impact on the accumulation rate of Hg in the surrounding soil. We estimated that the annual emission in the five phases of the smelter were 0.2 t, 4.3 t, 0.3 t, 0.5 t and 0.4 t, respectively. The total amount emitted and the total amount accumulated in the soil for each phase are also listed in Table 1. It can be seen that only 3%–15% of Hg emitted deposited locally and accumulated in the soil surrounding the smelter. During 1960–2011, 86% of Hg emitted went into the global pool, indicating that controlling Hg emissions from non-ferrous metal smelters is also important at a global scale.

The greatest impact of the smelter occurred from 1969 to 1990 when annual production increased from 20 kt Pb to 30 kt Pb plus 100 kt Zn.

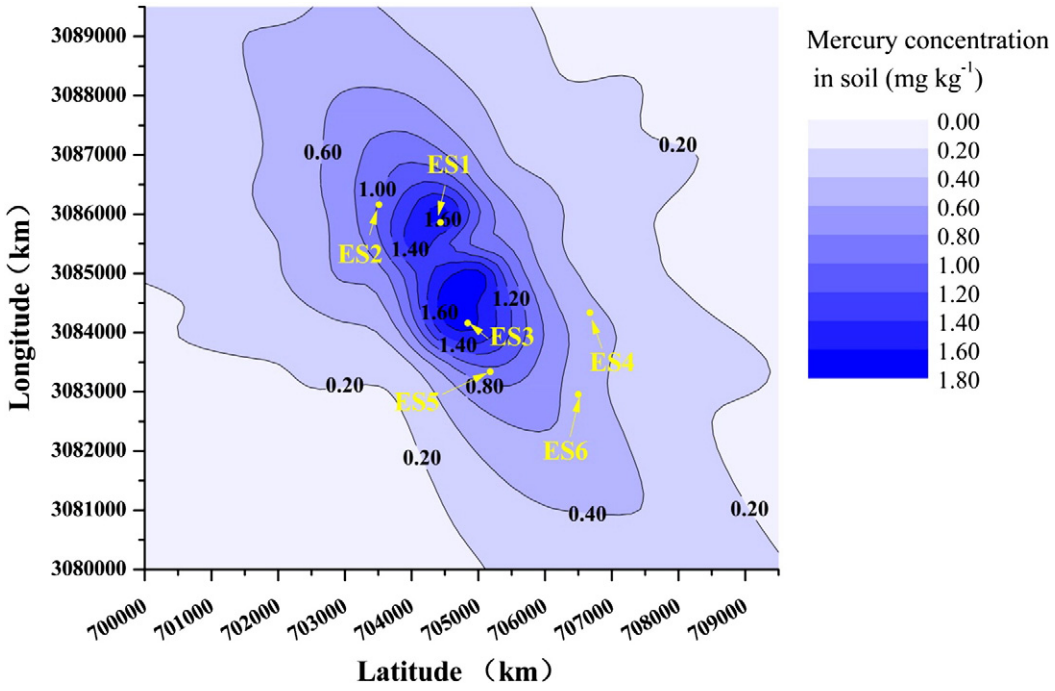

Fig. 5. Spatial concentrations of mercury in soil contributed by smelter emission generated by the model.

Although a dust collector (DC) was installed for the production change, the Hg removal efficiency (<10%) was unable to offset the increased emission caused by the larger production capacity. The annual Hg net deposition of 6450 μg m^{-2} yr^{-1} during this period had led to an increase of 0.40 mg kg^{-1} in soil Hg content (Fig. 6). In 1990, the average simulated concentration in the soil reached 0.41 mg kg^{-1}. The accumulation of Hg in soil slowed down during the period from 1991 to 2000 when the acid plants (AP) were installed and metal production capacity remained relatively constant. The implementation of the acid plant shifted the chemical speciation of Hg emission to RGM from 21% to 88% in the roasting process. The change in the emission speciation increased the efficiency of APCDs to ~99% and resulted in a much greater fraction of RGM emission that deposited near the emission source. In August of 2000 and July of 2005, two Hg reclaim towers (RT) were installed for controlling gaseous Hg emission, which further reduced the accumulation in soil. In 2011, the average simulated concentration in soil had reached 0.45 mg kg^{-1}. At the sites where soil Hg concentrations were measured, the average simulated concentration reached 1.46 mg kg^{-1}, 95% of the average measured concentration. Compared with the Hg concentration in Chinese background soil (0.04 mg kg^{-1}, Wei et al., 1991), the soil in our study domain is heavily polluted, posing a potential risk to the ecosystem and human health.

4. Conclusions

In this study, an integrated approach was developed to assess the input of Hg emission from large point sources to the soil. The model was applied to a Zn/Pb smelter in China and evaluated using the

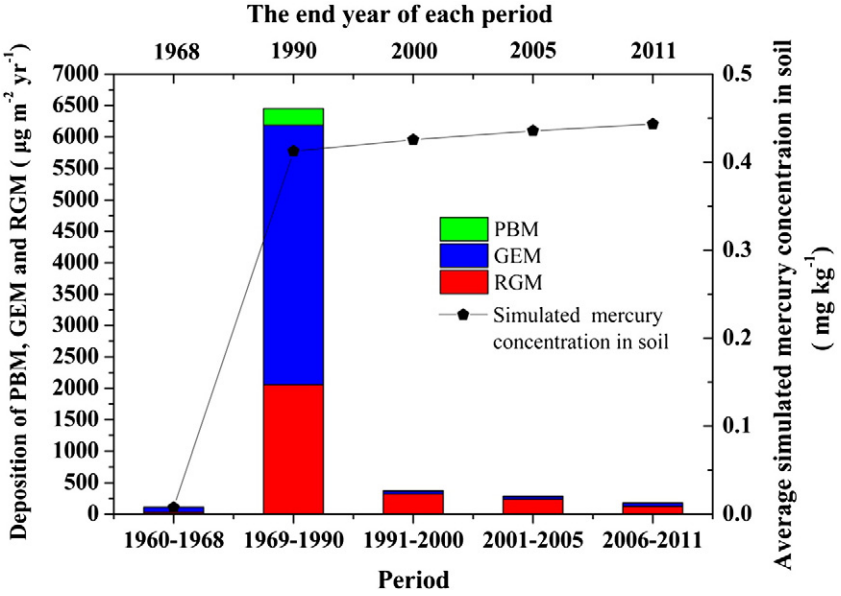

Fig. 6. Model simulated deposition of GEM, RGM and PBM in the different periods of smelter emissions associated with use of different pollution control devices and average simulated mercury concentration in soil at the end year of each period.

measurements of Hg in the atmosphere and soil. The degree of agreement between the simulated and observed soil Hg concentrations suggests that the model estimates for long-term accumulation from atmospheric deposition are conceivable.

From 1960 to 2011, the smelter emitted approximately 105 t of Hg into the atmosphere, resulting in 15 t of Hg net deposition within 5 km from the source. The deposition increased the Hg concentration in soil from 0.12 to 1.77 mg kg^{-1} in the study domain. The greatest impact of the smelter occurred from 1969 to 1990. The annual Hg net deposition of 6450 μg m^{-2} yr^{-1} during this period had led to an increase of 0.40 mg kg^{-1} in soil Hg content. From 1991 to 2011, atmospheric Hg emission from the smelter alone increased the average concentration in soil from 0.41 mg kg^{-1} to 0.45 mg kg^{-1}.

The integrated model developed in this study provides a useful approach for assessing the impacts of Hg emission from large point sources to the surrounding environment. The approach is also applicable to other heavy metals emitted from other large point sources. Application of this model in other areas and for other contaminants will further help evaluate the model performance and improve the method.

Acknowledgement

This work was funded by the 973 Program (No. 2013CB430001), the MEP's Special Funds for Research on Public Welfares (No. 201209015), and the Program for New Century Excellent Talents in University (NCET-10-0532). The authors also appreciate the support from the China Scholarship Council and China Project, School of Engineering and Applied Sciences of Harvard University.

References

Binkowski FS, Roselle SJ. Models-3 Community Multiscale Air Quality (CMAQ) model aerosol component 1. Model description. J Geophys Res 2003;108:4183–201.
Brus DJ, de Gruijter JJ. Random sampling or geostatistical modelling? Choosing between design-based and model-based sampling strategies for soil. Geoderma 1997;80(1–2):1–44.
Byun DW, Ching JKS. Science algorithms of the EPA models-3 Community Multiscale Air Quality (CMAQ) modeling system; 1999 [Washington D.C.].
Emery C, Tai E, Yarwood G. Enhanced meteorological modeling and performance evaluation for two Texas episodes. Report to the Texas Natural Resources Conservation Commission ENVIRON. California: International Corp Novato; 2001.
Ettler V, Rohovec J, Navratil T, Mihaljevic M. Hg distribution in soil profiles polluted by lead smelting. Bull Environ Contam Toxicol 2007;78:12–6.
Feng XB, Li GH, Qiu GL. A preliminary study on Hg contamination to the environment from artisanal zinc smelting using indigenous methods in Hezhang County, Guizhou, China: part 2. Hg contaminations to soil and crop. Sci Total Environ 2006;368:47–55.
Fu XW, Feng XB, Zhu WZ, Wang SF, Lu JL. Total gaseous Hg concentrations in ambient air in the eastern slope of Mt. Gongga, South-Eastern fringe of the Tibetan plateau, China. Atmos Environ 2008;42:970–9.
Fu XW, Feng XB, Dong ZQ, Yin RS, Wang JX, Yang ZR, et al. Atmospheric gaseous elemental Hg (GEM) concentrations and Hg depositions at a high-altitude mountain peak in south China. Atmos Chem Phys 2010;10:2425–37.
Gbor PK, Wen D, Meng F, Yang F, Zhang B, Sloan JJ. Improved model for Hg emission, transport and deposition. Atmos Environ 2006;40:973–83.
Kalac P, Burda J, Staskova I. Concentrations of lead, cadmium, Hg and copper in mushrooms in the vicinity of a lead smelter. Sci Total Environ 1991;105:109–19.
Kalac P, Niznanska M, Bevilaqua D, Staskova I. Concentrations of Hg, copper, cadmium and lead in fruiting bodies of edible mushrooms in the vicinity of a Hg smelter and a copper smelter. Sci Total Environ 1996;177:251–8.
Li GH, Feng XB, Li ZG, Qiu GL, Shang LH, Liang P, et al. Hg emission to atmosphere from primary Zn production in China. Sci Total Environ 2010;408:4607–12.
Li ZG, Feng XB, Li GH, Bi XY, Sun GY, Zhu JM, et al. Hg and other metal and metalloid soil contamination near a Pb/Zn smelter in east Hunan province, China. Appl Geochem 2011;26:160–6.
Lin C-J, Lindberg SE, Ho TC, Jang C. Development of a processor in BEIS3 for estimating vegetative Hg emission in the continental United States. Atmos Environ 2005;39:7529–40.
Lin Y, Vogt R, Larssen T. Environmental Hg in China: a review. Environ Toxicol Chem 2012;31:2431–44.
Liu HY, Jacob DJ, Yantosca RM. Constraints from Pb-210 and Be-7 on wet deposition and transport in a global three-dimensional chemical tracer model driven by assimilated meteorological fields. J Geophys Res Atmos 2001;106:12109–28.
Liu RH, Wang QC, Lu XG, Fang FM, Wang Y. Distribution and speciation of Hg in the peat bog of Xiaoxing'an Mountain, northeastern China. Environ Pollut 2003;124:39–46.
Liu XD, Zhao SP, Sun LG, Yin XB, Xie ZQ, Honghao L, et al. P and trace metal contents in biomaterials, soils, sediments and plants in colony of red-footed booby (Sula sula) in the Dongdao Island of South China Sea. Chemosphere 2006;65:707–15.
Liu Y, Ye C, Li W. Research and application of regional irrigation amount forecast for cropland based on RS and GIS. J Nat Resour 2012;27:1061–9.
Lonati G, Zanoni F. Monte-Carlo human health risk assessment of Hg emissions from a MSW gasification plant. Waste Manag 2013;33:347–55.
MEP (Ministry of Environmental Protection of the People's Republic of China). Technical methods for making local emission standards of air pollutants (GB/T 13201-91); 1991 [Beijing].
Rieuwerts JS, Farago M. Hg concentrations in a historic lead mining and smelting town in the Czech Republic: a pilot study. Sci Total Environ 1996;188:167–71.
Scire JS, Strimaitis DG, Yamartino RJ. In: Report for California Air Resources Board-Model formulation and user's guide for the Calpuff dispersion model; 1990 [California].
Streets DG, Bond TC, Carmichael GR, Feamdes SD, Fu Q, He D, et al. An inventory of gaseous and primary aerosol emissions in Asia in the year 2000. J Geophys Res 2003;108:8809–31.
Streets DG, Hao JM, Wu Y, Jiang JK, Chan M, Tian HZ, et al. Anthropogenic Hg emissions in China. Atmos Environ 2005;39:7789–806.
Svoboda L, Zimmermannova K, Kalac P. Concentrations of Hg, cadmium, lead and copper in fruiting bodies of edible mushrooms in an emission area of a copper smelter and a Hg smelter. Sci Total Environ 2000;246:61–7.
UNEP (United Nations Environment Programme)Technical background report for the global Hg assessment; 2013. [Geneva].
US EPA (United States Environmental Protection Agency)Hg study report to congress; 1997. [Washington, D.C.].
US EPA (United States Environmental Protection Agency)AERMOD: Description of model formulation; 2004. [Washington, D.C.].
US EPA (United States Environmental Protection Agency). Human health risk assessment for hazardous waste combustion facilities; 2005 [Washington, D.C.].
Wan Q, Feng XB, Lu J, Zheng W, Song XJ, Han SJ, et al. Atmospheric Hg in Changbai Mountain area, northeastern China I: the seasonal distribution pattern of total gaseous Hg and its potential sources. Environ Res 2009;109:201–6.
Wang D. Hydrogeology foundation. Geological PublisherBeijing: Geological Publisher; 1995.
Wang D. Practical technology for impact assessment atmospheric environment. Standards Press of ChinaBeijing: Standards Press of China; 2010.
Wang SX, Liu M, Jiang JK, Hao JM, Wu Y, Streets DG. Estimate the Hg emissions from non-coal sources in china. Environ Sci (Chin) 2006;27:2401–6.
Wang XD, Cheng GW, Zhong XH, Li MH. Trace elements in sub-alpine forest soils on the eastern edge of the Tibetan Plateau, China. Environ Geol 2009;58:635–43.
Wang SX, Song JX, Li GH, Wu Y, Zhang L, Wan Q, et al. Estimating Hg emissions from a zinc smelter in relation to China's Hg control policies. Environ Pollut 2010;158:3347–53.
Wei FS, Chen JS, Wu YY, Zheng CJ. Background value of Chinese soil element. Environ Sci (Chin) 1991;12:12–9.
Wesely M. Parameterization of surface resistances to gaseous dry deposition in regional-scale numerical models. Atmos Environ 1989;23:1293–304.
Wu Y, Wang SX, Streets DG, Hao JM, Chan M, Jiang JK. Trends in Anthropogenic Mercury Emissions in China from 1995 to 2003. Environ Sci Technol 2006;40:5312–8.
Wu QR, Wang SX, Zhang L, Song JX, Yang H, Meng Y. Update of mercury emissions from China's primary zinc, lead and copper smelters, 2000–2010. Atmos Chem Phys 2012;12:11153–63.
Yin XB, Yao CX, Song J, Li ZB, Zhang CB, Qian W, et al. Hg contamination in vicinity of secondary copper smelters in Fuyang, Zhejiang Province, China: levels and contamination in topsoil. Environ Pollut 2009;157:1787–93.
Zhang XPP, Deng W, Yang XMM. The background concentrations of 13 soil trace elements and their relationships to parent materials and vegetation in Xizang (Tibet), China. J Asian Earth Sci 2002;21:167–74.
Zhang L, Blanchard P, Johnson D, Dastoor A, Ryzhkov A, Lin C, et al. Assessment of modeled Hg dry deposition over the Great Lakes region. Environ Pollut 2012a;161:272–83.
Zhang L, Wang SX, Wu QR, Meng Y, Yang H, Wang FY, et al. Were Hg emission factors for Chinese non-ferrous metal smelters overestimated? Evidence from onsite measurements in six smelters. Environ Pollut 2012b;171C:109–17.
Zheng N, Liu JS, Wang QC, Liang ZZ. Hg contamination due to zinc smelting and chlor-alkali production in NE China. Appl Geochem 2011;26:188–93.